



MARMARA UNIVERSITY
FACULTY OF ENGINEERING



**EXPERIMENTAL AND NUMERICAL
INVESTIGATION OF THE EFFECT OF
NANOMATERIAL REINFORCEMENT ON
MECHANICAL PROPERTIES
IN THERMOSET MATRIX COMPOSITES**

Görkem Özkan, Furkan Giray Özkan, Mustafa Emre Altıntaş

GRADUATION PROJECT REPORT
Department of Mechanical Engineering

Supervisor
Asst. Prof. AYBALA YILDIRIM

ISTANBUL, 2024



MARMARA UNIVERSITY
FACULTY OF ENGINEERING



**Experimental and Numerical Investigation of
the Effect of Nanomaterial
Reinforcement on Mechanical Properties
in Thermoset Matrix Composites**

by

Görkem Özkan, Furkan Giray Özkan, Mustafa Emre Altıntaş

June 26, 2024, Istanbul

**SUBMITTED TO THE DEPARTMENT OF MECHANICAL
ENGINEERING IN PARTIAL FULFILLMENT OF THE
REQUIREMENTS FOR THE DEGREE**

OF

BACHELOR OF SCIENCE

AT

MARMARA UNIVERSITY

The author(s) hereby grant(s) to Marmara University permission to reproduce and to distribute publicly paper and electronic copies of this document in whole or in part and declare that the prepared document does not in any way include copying of previous work on the subject or the use of ideas, concepts, words, or structures regarding the subject without appropriate acknowledgement of the source material.

Signature of Author(s)

Department of Mechanical Engineering

Certified By

Project Supervisor, Department of Mechanical Engineering

Accepted By

Head of the Department of Mechanical Engineering

ACKNOWLEDGEMENT

First and foremost, we would like to express our gratitude to Asst. Prof. Aybala YILDIRIM, our supervisor, for her help and guidance during the preparation of this thesis.

We are very grateful to Asst. Prof. Muhammet CEYLAN for allowing us to use his laboratory and equipment at Istanbul Ticaret University.

We would like to express our gratitude to Prof. Dr. Paşa YAYLA for graciously accepting our need of help to make test to our specimens.

June, 2024

Görkem Özkan, Furkan Giray Özkan,
Mustafa Emre Altıntaş

CONTENTS

ACKNOWLEDGEMENT	ii
CONTENTS.....	iii
ABSTRACT.....	iv
SYMBOLS.....	v
LIST OF FIGURES	vii
LIST OF TABLES	viii
1.INTRODUCTION	1
1.1.Literature Review.....	1
2.MATERIALS AND METHODS	3
2.1. Materials	4
2.2. Optimization of Ply Orientation.....	5
2.3. Production Methods.....	7
2.3.1.Vacuum bagging method	7
2.3.2.Production of specimens	7
2.4. Test Methods.....	11
2.4.1.Tensile test	11
2.4.2.Charpy Impact Test.....	13
3.RESULTS & DISCUSSION.....	14
3.1. Tensile Test Results	14
3.2. Theoretical Results of Tensile Properties	18
3.3. Charpy Impact Test Results	21
4.FEASIBILITY & COST ANALYSIS.....	24
5.CONCLUSION & FUTURE WORKS	25
6.REFERENCES	26
7APPENDIX.....	28

ABSTRACT

Composite materials are materials made by combining at least two different substances (matrix and fiber). Due to their attractive mechanical properties, such as durability, light weight, and strength, they are frequently used in the automotive and aerospace industries, construction industry, sports equipment, electronics, and other fields.

Nanoparticles are particles on the nanoscale that can alter both the chemical and physical properties of the material they are added to. Due to their small size, they have a large surface area, which significantly impacts their chemical and physical properties. Nanoparticles are often used in composites to modify their mechanical properties.

In this project, the mechanical properties of carbon fiber-epoxy composites with various ratios of SiO₂ and TiO₂ nano-particles in their matrices produced from 9 sheets in the form of hand loops are compared. The specimens to be tested within the scope of the project were produced, two for each composite with different matrix. These specimens were produced in accordance with ASTM-D638 and ASTM E23 standards and tensile and Charpy impact tests were applied. Composite plates with four different particle ratios by mass were produced (0%, 1%, 2%, 4%). Tensile Strength and Impact Strength data resulting from the tests were compared and reported.

The aim of this project is to observe and examine how the mechanical properties of the composite material we produce are affected when nanoparticles composed of a mixture of SiO₂ and TiO₂ are added to the composite in different ratios, and to understand how these mechanical properties change. To examine these effects, tensile test and Charpy impact test were performed.

SYMBOLS

- mm** : Millimeter
µm : Micrometer
g : Gram
g/cm³ : Gram per cubic centimeter
kN : Kilonewton
B : Width
t : Thickness
A : Cross-sectional Area
σ : Stress
σ_{ut} : Ultimate tensile strength
ε : Strain
ε_{ut} : Ultimate tensile strain
F_{max} : Max force
δ_{max} : Maximum displacement
L_g : Gage length
E : Elastic Modulus
C_{VN} : Charpy Impact Strength
GPa : Gigapascal
Mpa : Megapascal

ABBREVIATIONS

ASTM	: American Society for Testing and Materials
CF/Ep	: Carbon Fabric Reinforced Epoxy
CFRP	: Carbon Fiber Reinforced Plastic
GFRP	: Glass Fiber Reinforced Plastics
SiO₂	: Silicon Dioxide
TiO₂	: Titanium dioxide

LIST OF FIGURES

Figure 2.1 Strength Ratios of Each Laminate.....	6
Figure 2.2 Schematic diagram of vacuum bagging	7
Figure 2.3. Carbon fiber fabric measurements	8
Figure 2.4. Applying epoxy hardener mixture on each event.....	9
Figure 2.5. Applying vacuum to the composite plate in a bag	9
Figure 2.6. Weighing of nanoparticles to be mixed with epoxy on a sensitive scale	10
Figure 2.7 Application of sonication process of epoxy nanoparticle mixture	10
Figure 2.8. Composite with 1% nanoparticles by mass.....	11
Figure 2.9. Tensile test specimens and their clip gage in the indicator	12
Figure 2.10. The setup of the tensile test.....	12
Figure 2.11. Specimens that are tested in charpy impact test	13
Figure 3.1. Composite No-4 Stress-Strain Graph (a) Sample 1; (b) Sample 2.....	14
Figure 3.2. Composite No-3 Stress-Strain Graph (a) Sample; 1 (b) Sample 2.....	15
Figure 3.3. Composite No-2 Stress-Strain Graph (a) Sample 1; (b) Sample 2.....	15
Figure 3.4. Composite No-1 Stress-Strain Graph Sample 1.....	15
Figure 3.5. Average values of tensile strength properties of each composite.....	17
Figure 3.6. Composite No-4 Time vs Force and Energy Graph (a) Sample 1; (b) Sample 2.....	22
Figure 3.7. Composite No-3 Time vs Force and Energy Graph (a) Sample 1; (b) Sample 2.....	22
Figure 3.8. Composite No-2 Time vs Force and Energy Graph (a) Sample 1; (b) Sample 2.....	22
Figure 3.9. Composite No-1 Time vs Force and Energy Graph (a) Sample 1; (b) Sample 2.....	22
Figure 3.10 Average values of impact strength properties of each composite.....	23

LIST OF TABLES

Table 2.1. Physical properties of the epoxy resin	4
Table 2.2. Physical properties of the hardener	4
Table 2.3. Properties of Carbon Fiber Fabric	4
Table 2.4. Properties of SiO ₂	4
Table 2.5. Properties of TiO ₂	5
Table 2.6. Different angle orientations according to types.....	5
Table 2.7. Strength Ratios of Laminate a Plies	6
Table 2.8. Sample composition and mass % ratios	8
Table 3.1. Tensile strength validation of Composite No-4.....	15
Table 3.2. Tensile strength validation of Composite No-3.....	15
Table 3.3. Tensile strength validation of Composite No-2.....	15
Table 3.4. Tensile strength validation of Composite No-1.....	16
Table 3.5 Mechanical Properties of Epoxy/Carbon Fiber Composite.....	18
Table 3.6. Midplane Strains and Curvatures.....	18
Table 3.7. Elastic Constants for this laminate.....	18
Table 3.8. Global Stresses (Pa)	19
Table 3.9. Global Strains.....	19
Table 3.10. Local Stresses (Pa)	20
Table 3.11. Local Strains.....	20
Table 3.12. Impact strength validation of Composite No-4.....	22
Table 3.13. Impact strength validation of Composite No-3.....	23
Table 3.14. Impact strength validation of Composite No-2.....	23
Table 3.15. Impact strength validation of Composite No-1.....	23
Table 4.1. Cost analysis of the project.	24

1. INTRODUCTION

Advancements in the fields of engineering and materials science continue to progress rapidly. These advancements are also evident in the area of composite materials. Innovations in composite materials have enabled the development of new composites with superior properties. Among these innovations, thermoset matrix composites reinforced with nanomaterials are garnering significant interest due to their potential applicability in various industrial sectors such as aerospace, automotive, and construction, owing to their superior mechanical performance [1,2]. This thesis aims to investigate the effect of adding specific nanoparticles to composites on the mechanical properties of the composite [3]. In this research, silicon dioxide (SiO_2) and titanium dioxide (TiO_2) will be used as nanoparticles.

Thermoset polymers are polymers obtained by the irreversible curing of a soft solid or viscous liquid pre-polymer [4]. Due to their excellent thermal stability and structural integrity, they are widely used as matrices in composite materials. However, the brittle nature and limited mechanical strength of these polymers can pose challenges in some high-performance applications. In the composite used in this research, carbon-fiber is utilized as the thermoset matrix [5,6]. The inclusion of nanomaterials into thermoset matrices can enhance mechanical properties, offering a solution to limitations such as brittleness. Due to their high surface area-to-volume ratios and superior physical properties, nanoparticles can significantly improve mechanical properties such as tensile strength, flexural strength, and impact resistance of composites [7].

Effect of nano-silicon dioxide on mechanical properties of carbon fiber reinforced epoxy composites G.S. Researched by Divya and B. Suresha. Amine-containing liquid rubber was added to the epoxy matrix to increase SiO_2 dispersion. The SiO_2 was then mixed thoroughly using an ultra-sonication method [8]. The production of carbon fabric reinforced epoxy (CF/Ep) composite with surface treated nano- SiO_2 was carried out by hot pressing and vacuum bagging [9]. Following ASTM guidelines, the impact of silane-treated nano- SiO_2 on static mechanical parameters including hardness, tensile, and flexural qualities was evaluated at different filler loading of 0.5%, 1%, and 3% by weight [8]. The interfacial bonding between nano- SiO_2 particles and epoxy resin is increased by the addition of silane coupling agent, according to experimental data, which enhances the surface hardness, tensile, and bending characteristics. Furthermore, it was observed that CF/Ep composites with 3 weight percent nano- SiO_2 filler had a greater void content [8]. (G.S. Divya, B. Suresha, 2021)

Silicon dioxide (SiO_2) nanoparticles are notable for their exceptional hardness, chemical stability, and thermal resistance. Various previous studies have demonstrated the

capability of these nanoparticles to enhance the mechanical properties of composites, making them an ideal choice for reinforcement [10]. On the other hand, titanium dioxide (TiO_2) nanoparticles are known for their high tensile strength, corrosion resistance, and photocatalytic properties [11]. It is hypothesized that the combined use of SiO_2 and TiO_2 nanoparticles in different proportions within thermoset matrices will enhance the mechanical performance of the composites.

Impact damage in SiO_2 nanoparticle enhanced epoxy - Carbon fiber composites was examined by M. Landowski et al. Using industrial surface modified nano silicas, the epoxy resin matrix was reinforced with SiO_2 nanoparticles from 1% to 8% by weight. Impact parameters, force, deformation, energy and damage extent were recorded. The most obvious effect among these parameters is the reduction in damage size. As an example, a 28% reduction was recorded by infrared thermography and X-ray computational radiography for the composite containing 8% nano SiO_2 . Crack branching and crack deflection caused by nanoparticles were observed. Around 15% permanent deformation and 8% reduction in energy absorption were observed, along with an increase in fiber/matrix interface strength. The flexural strength peaked at 640 MPa at 2-5% nano- SiO_2 content and decreased thereafter, which was probably attributed to nanoparticle agglomerations. A 6% increase in peak impact force was recorded in the composite containing 8% nano- SiO_2 . The onset of reduction in maximum power and impact damage size was revealed for 5% nano- SiO_2 . An impressive 28% damage size reduction was observed in the composite containing 8% nano- SiO_2 . The lack of previous reports of such a large damage size reduction for glass fiber reinforced plastic (GFRP) and carbon fiber reinforced plastic (CFRP) laminates has been attributed to energy absorption mechanisms provided by crack deflection and crack branching triggered by nanoparticle agglomerates [12].

In this research, the effect of adding a mixture of SiO_2 and TiO_2 (with the ratio of SiO_2 to TiO_2 being equal) in different proportions to various samples on the mechanical properties of thermoset matrix composites will be examined. Through experimental investigations such as tensile testing and impact testing, mechanical properties like tensile strength and impact resistance will be analyzed, providing a comprehensive understanding of how to optimize nanomaterial reinforcement for superior performance.

This study aims to contribute to the development of high-performance composite materials by elucidating the effects of SiO_2 and TiO_2 nanoparticles on the mechanical properties of thermoset matrix composites. In this context, it is intended to provide significant insights into how nanomaterial-enhanced composites can be utilized in future applications.

In the materials and methods section will detail the preparation of the composites and the test procedures used. The findings and discussion section will present and interpret the obtained results, and the conclusion will summarize these findings and offer recommendations for future research.

1.1. Literature Review

In this study, nano titanium dioxide (TiO_2) particles were added to the epoxy matrix carbon fiber composite at the rates of 0%, 2%, 4% and 6% by mass. Impact resistance and wear resistance tests were carried out on the created samples. Carbon fibers have a more brittle structure than other synthetic fibers. For this reason, their use is limited in applications requiring high impact resistance. However, with the addition of TiO_2 particles, a significant improvement in impact strength was observed in the composites. The addition of nanoparticles filled the cavities inside the samples and increased the adhesion between the epoxy and fiber material. As a result of the tests, it was seen that the addition of TiO_2 increased the mechanical properties of the composites. Composite samples with 4% nano TiO_2 particles showed the highest improvement [13].

In this study, SiO_2 nanoparticles were mixed with epoxy fiber glass composites in various proportions. Composite samples produced by mixing SiO_2 particles at 0%, 1%, 3% and 5% by mass were then subjected to tensile testing. It was observed that the addition of nanoparticles increased the adhesion force between the fibers and the matrices and increased the mechanical properties of the samples. Among the samples with SiO_2 added, the sample with 1% had the highest tensile strength. In addition, samples with higher proportions of particles formed aggregation in the matrix and caused a decrease in the strength of the materials. In the study, composites with plies arranged in different orientations were compared and higher tensile strength was observed in composites with plies parallel to the tensile direction [14].

Previous studies have shown that SiO_2 and TiO_2 nanoparticles improve the mechanical properties of composite materials. In this study, considering the impact resistance improvement of TiO_2 particles on the composite and the positive effect of SiO_2 on tensile strength, it is expected that the combined effect of these two particles will provide a two-sided improvement in a composite material to be produced.

2. MATERIALS AND METHODS

Carbon fiber epoxy composites have a wide range of uses in industrial and engineering applications with their excellent combination of strength and lightness. The mechanical

properties of these composites can be optimized with nanoscale additives in the epoxy matrix. Nanoparticles such as TiO₂ and SiO₂ can increase the mechanical strength of the composite, and when these nanoparticles are distributed homogeneously within the composite, they increase the strength of the composite. The high surface area of nanoparticles strengthens the interaction of the composite with its matrix and increases the fatigue strength of the material by preventing crack formation. It can also improve wear resistance. The addition of these additives allows the composite to maintain its lightness while improving its performance.

2.1. Materials

In this study, MGS LR285 is the epoxy resin, MGS LH285 is the hardener, and nanoparticles are SiO₂ and TiO₂.

Table 2.1. Physical properties of the epoxy resin

Epoxy Resin MGS LR285	
Density [g/cm ³]	1.18-1.23
Viscosity [mPa·s]	600-900
Refractory index	1.525-1.530

Table 2.2. Physical properties of the hardener

Curing Agent MGS LH285	
Density [g/cm ³]	0.94-0.97
Viscosity [mPa·s]	50-100
Refractory index	1.500-1.510

Measuring conditions: measured at 25°. (Momentive Specialty Chemicals) 300g/m² unidirectional carbon fiber fabric was used.

Table 2.3. Properties of Carbon Fiber Fabric

Carbon Fiber Fabric	
Resin Consumption	346 g / m ²
Laminate Thickness	0.48 mm
Laminate Weight	646 g / m ²

Table 2.4. Properties of SiO₂

Silicon Dioxide 10 μm

Density	2.65 g/cm ³
Melting point	1.710 °C:
Boiling point	2.230 °C

Table 2.5. Properties of TiO₂

Titanium Dioxide 0.405 μm	
Density	4.23 g/cm ³
Melting point	1.843 °C
Boiling point	2.972 °C

2.2. Optimization of Ply Orientation

To achieve the best results from the tensile and impact tests we will perform, the plies in the laminates we prepare must be arranged with the most suitable orientation. To ensure this:

- The plies should be stacked symmetrically with respect to the mid-plane to provide a stable laminate structure.
- To achieve high elastic modulus in both the x and y directions, the plies should be placed at 90°, 0°, and 45° angles.
- Plies with the same angle should not be placed consecutively.

Considering these conditions, laminates with different ply orientations were tested in MATLAB with code in Appendix according to the Tsai-Wu criteria by applying a 1 kN tensile force in the y direction (that is, the direction parallel to the fibers in the 0° ply) [15].

Table 2.6. Different angle orientations according to types

Types	Orientations
A	[0° / +45° / -45° / 90° / 0° / 90° / -45° / +45° / 0°]
B	[90° / +45° / -45° / 0° / 90° / 0° / -45° / +45° / 90°]
C	[-45° / 0° / +45° / 90° / -45° / 90° / 45° / 0° / -45°]
D	[0° / -45° / 90° / +45° / 0° / +45° / 90° / -45° / 0°]
E	[-45° / 90° / +45° / 0° / -45° / 0° / +45° / 90° / -45°]
F	[90° / -45° / 0° / +45° / 90° / +45° / 0° / -45° / 90°]
G	[+45° / -45° / 90° / 0° / +45° / 0° / 90° / -45° / +45°]
H	[90° / -45° / 0° / +45° / 90° / +45° / 0° / -45° / 90°]

- I $[0^\circ / +45^\circ / 90^\circ / -45^\circ / 0^\circ / -45^\circ / 90^\circ / +45^\circ / 0^\circ]$
J $[+45^\circ / 0^\circ / 90^\circ / -45^\circ / +45^\circ / -45^\circ / 90^\circ / 0^\circ / +45^\circ]$

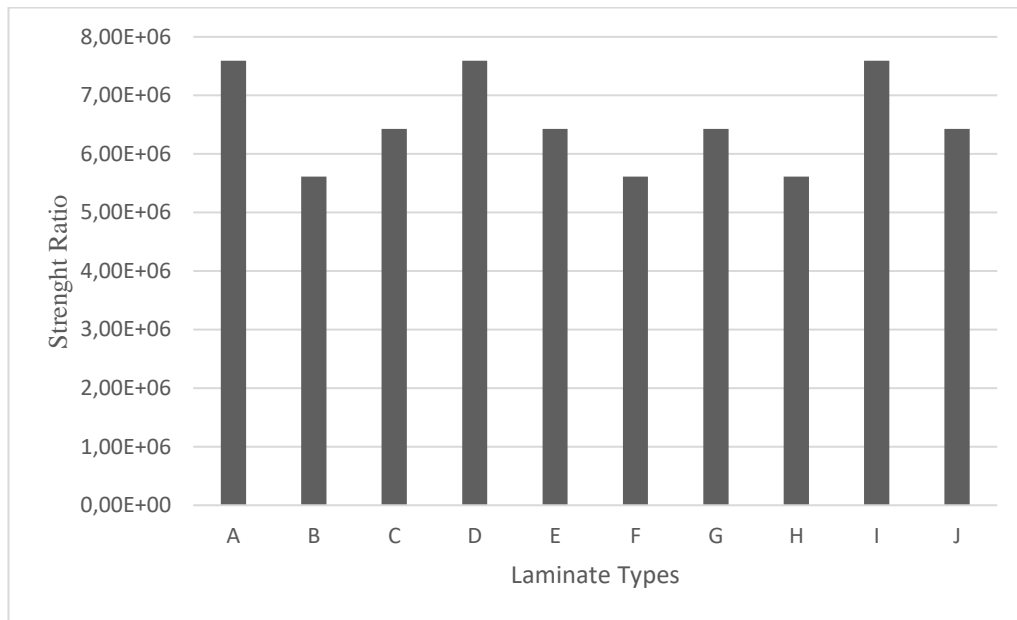


Figure 2.1 Strength Ratios of Each Laminate

Since the strength ratios of the tested samples resulted in constant values, further iterations will be unnecessary. Considering the strength ratios and the ease of production of the laminates, laminate A was found to be the most suitable for production. (The Tsai-Wu failure criteria were applied to all plies of each laminate, and the ply with the highest SR value was selected.)

Table 2.7. Strength Ratios of Laminate a Plies

Ply no.	Position	Tsai-Wu
1 (0°)	Top	0.759×10^7
	Bottom	0.759×10^7
2 ($+45^\circ$)	Top	0.317×10^7
	Bottom	0.317×10^7
3 (-45°)	Top	0.317×10^7
	Bottom	0.317×10^7
4 (90°)	Top	0.366×10^7
	Bottom	0.366×10^7
5 (0°)	Top	0.759×10^7
	Bottom	0.759×10^7
6 (90°)	Top	0.366×10^7
	Bottom	0.366×10^7
7 (-45°)	Top	0.317×10^7
	Bottom	0.317×10^7
8 ($+45^\circ$)	Top	0.317×10^7
	Bottom	0.317×10^7

9 (0°)	Bottom	0.317×10^7
	Top	0.759×10^7
	Bottom	0.759×10^7

In Table-2.7, using the Tsai-Wu theory, it was observed that the plies with the lowest strength ratios were those oriented at 90°.

2.3. Production Methods

2.3.1. Vacuum bagging method

During the curing phase, the laminate is placed under mechanical pressure using vacuum bagging. Applying pressure to composite laminates can provide many benefits. First, it eliminates air trapped between layers. Secondly, it maintains the alignment of the fibers during curing and compresses the fiber layers to ensure effective force transfer between fiber bundles. Third, it reduces humidity. Most importantly, vacuum bagging optimizes the fiber-to-resin ratio in the composite part. These advantages have long allowed the racing and aerospace industries to improve the physical properties of advanced composite materials such as carbon, aramid, and epoxy [16-18].

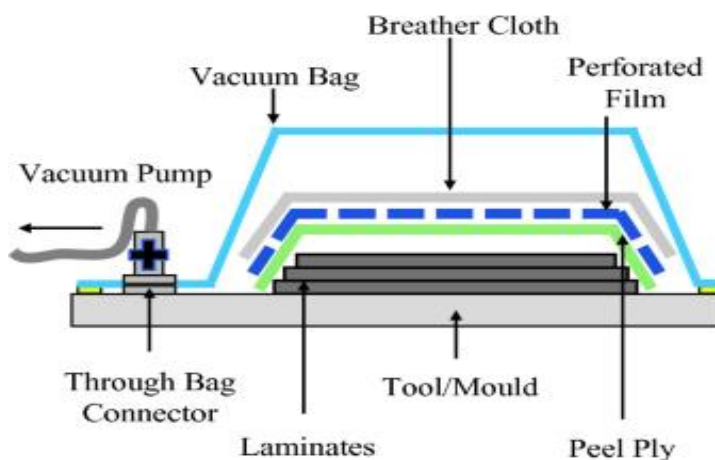


Figure 2.2 Schematic diagram of vacuum bagging

2.3.2. Production of specimens

In this study, 4 different composite specimens were prepared. Nanoparticles were added to the epoxy resin chosen as the matrix at ratios of %0.5 SiO₂ +%0.5TiO₂, %1 SiO₂ + %1SiO₂ and %2SiO₂ + %2TiO₂. In addition to this, one of the specimens was prepared without the addition of nanoparticles. In the bellow table, the materials and nanoparticle amounts used in each specimen prepared are given.

Table 2.8. Sample composition and mass % ratios

Composite No	Epoxy	Carbon Fiber	SiO ₂	TiO ₂	Total Mass(g)
1	54.79%	45.21%	0	0	161.37
2	54.24%	44.76%	0.5%	0.5%	163
3	53.70%	44.30%	1%	1%	164.63
4	52.60%	43.40%	2%	2%	168.09

Many steps in production until the final product are examined and followed carefully.

Firstly, the carbon fiber fabric was cut to appropriate sizes as shown in Figure-2.3. The 130 mm² fabric in the image is for 0- and 90-degree plies, while the 195mm² fabric is for 45-degree plies.

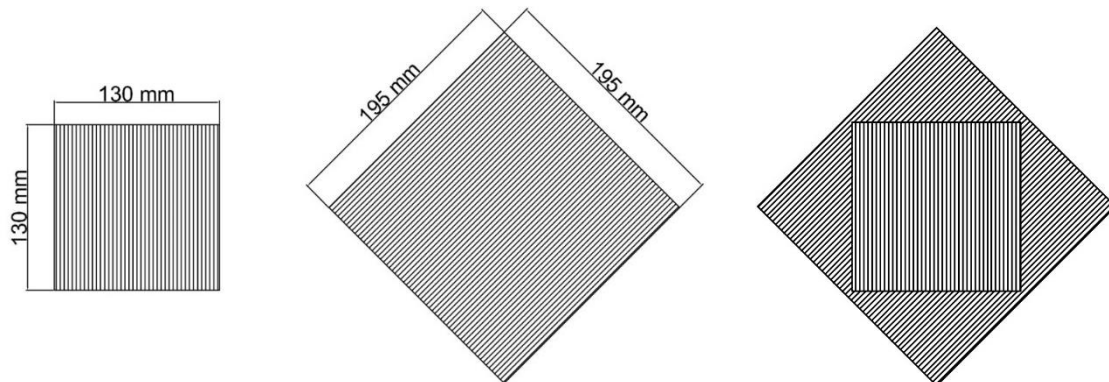


Figure 2.3. Carbon fiber fabric measurements

For the composite without nanoparticles, the first step is to mix the epoxy resin and hardener in a ratio of 2 parts epoxy to 1 part hardener (29.47 g hardener + 58.94 g epoxy resin). The cut carbon fiber fabrics are laid out appropriately on the metal table. The prepared mixture is applied appropriately to each layer of the carbon fiber, completing 9 layers in total.

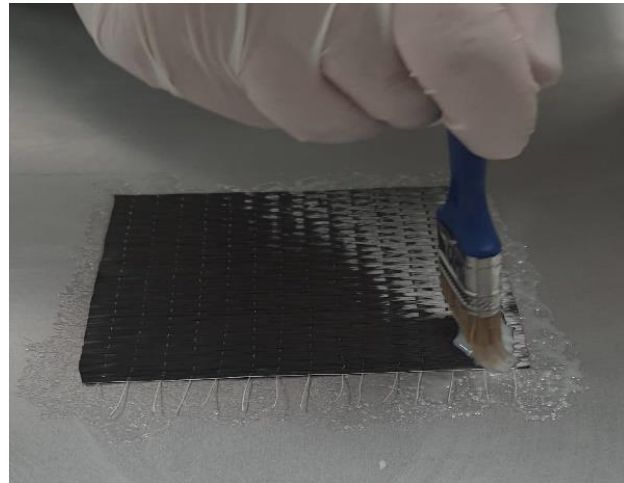


Figure 2.4. Applying epoxy hardener mixture on each event

Then, Peel ply is placed on top. The rough texture of the Peel ply allows the removal of air or other VOCs from the part via vacuum during hand lay-up or infusion applications. Therefore, Peel ply is commonly used in vacuum hand lay-up, infusion, or prepreg applications. Felt is placed on top of the Peel ply to absorb excess epoxy. As the final step, the vacuum bag is properly positioned and sealed to the surface with sealing tape. This initiates the vacuuming process, which runs for approximately 3 hours. Then, system is left to cure for 24 hours.

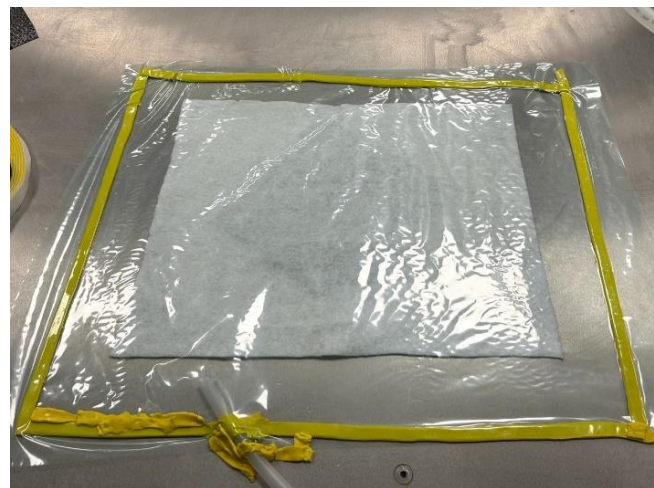


Figure 2.5. Applying vacuum to the composite plate in a bag

For nanoparticle-reinforced composite materials, the necessary weight of nanoparticles was first individually weighed using a precision balance.

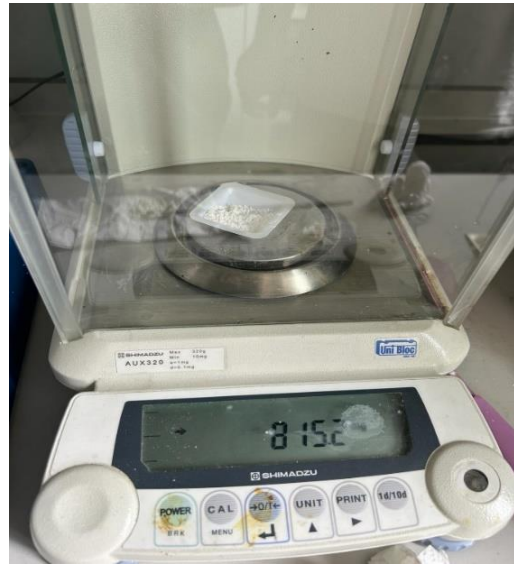


Figure 2.6. Weighing of nanoparticles to be mixed with epoxy on a sensitive scale

Then, the mixture combined with resin was sonicated in a WiseClean WUC A22H Ultrasonic Bath device. Sonication helps to homogenize the mixture, remove air bubbles, reduce viscosity, accelerate curing, and enhance the functionality of the nanoparticles. These processes enable better dispersion of the nanoparticles within the epoxy matrix and improve the mechanical properties of the composite.



Figure 2.7 Application of sonication process of epoxy nanoparticle mixture

Then, the hardener is added and mixed, and the same processes are repeated to make composite. After being vacuumed for 3 hours, it is left to cure for 24 hours.

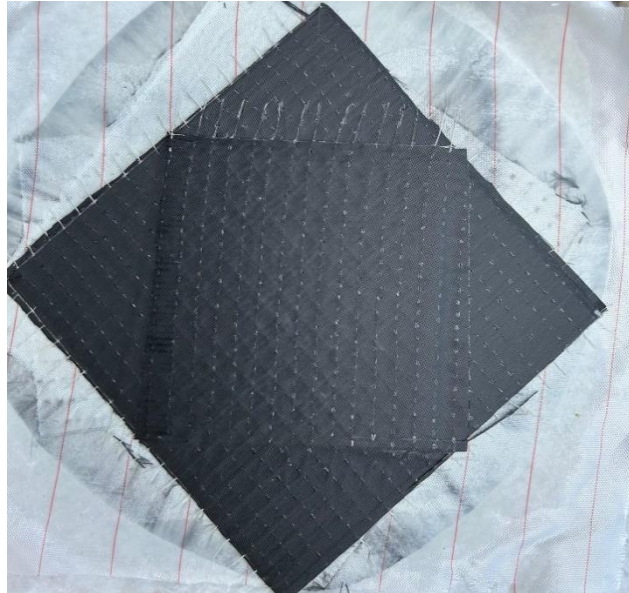


Figure 2.8. Composite with 1% nanoparticles by mass

2.4. Test Methods

Mechanical tests are performed to measure the physical properties of materials and to create a certain standard from these properties. Although these tests were in various numbers to find different properties, in this project, we did the tensile test to find the Tensile Strengths and Young's modulus of the composite we produced, and the Charpy impact test to find the impact strength. Then, we compared the results of the Tensile Strength test with the results of the MATLAB code we wrote.

2.4.1. Tensile test

Tensile testing is used to measure the force required to break a composite specimen and how much the specimen stretches or elongates to that point of fracture. We can find Yield Strength, Ultimate Tensile Strength and Young's Modulus with the stress-strain diagram we took from the tensile test diagram. Based on the resulting data, parts are designed to withstand the applied force [20].

In this study, the ultimate tensile strength, strain at the ultimate strength point and elastic modulus of carbon/epoxy composites were investigated by tensile test. For the tensile test, specimens containing 1%, 2% and 4% nanoparticles by weight and specimens without nanoparticles were investigated.



Figure 2.9. Tensile test specimens and their clip gage in the indicator

The test was completed by using SHIMADZU testing machine according to ASTM D638. The specimens were rectangular in shape with a length of 115 mm, a width of 19 mm and 3 mm thicknesses. A typical test speed of 2.5 mm/min is applied for test specimens is shown in Figure-2.10 [21].



Figure 2.10. The setup of the tensile test

In tensile testing, some calculations are required for stress, strain and elastic modulus. Accordingly, certain formulas are used for calculations.

To calculate the tensile modulus, Equation (2.1) is used.

$$\sigma_{ut} = \frac{F_{max}}{A} \quad (2.1)$$

where:

σ_{ut} = ultimate tensile strength, MPa

F_{max} = max force point at data

A = cross-sectional area, mm²

To calculate the ultimate tensile strain, the maximum displacement before the failure is required. Then, it can be calculated using Equation (2.2).

$$\varepsilon_{ut} = \frac{\delta_{max}}{L_g} \quad (2.2)$$

where:

ε_{ut} = ultimate tensile strain, mm/mm

δ_{max} = maximum displacement before failure, mm

L_g = gage length, mm

To calculate the modulus of elasticity (Young Modulus), Equation (2.3) is used.

$$E = \frac{\sigma}{\varepsilon} \quad (2.3)$$

2.4.2. Charpy Impact Test

Charpy Impact test is used to find out how materials act on impact energy. With this test we can learn materials fracture strength, ductility and brittleness. Charpy impact test measures the notch sensitivity and also helps to create standards for material behaviors.

The test was carried out using INSTRON impact pendulum according to ASTM E23. The specimens were rectangular in shape with a length of 55 mm, a width of 10 mm and 3 mm thicknesses and 2 mm notch length. 3.799 m/s impact velocity and 15 J potential hammer energy are applied for test specimens.



Figure 2.11. Specimens that are tested in charpy impact test

In impact testing, some calculations are required for stress, strain and elastic modulus. Accordingly, certain formulas are used for calculations.

To calculate the Charpy Impact Strength,

$$C_{VN} = \frac{E}{(B-a)t} \times 10^3 \quad (2.4)$$

Where:

B: Width of the specimen (mm)

a: Notch length of specimen (mm)

t: Thickness of specimen (mm)

E: Absorbed Energy (Joule)

3. RESULTS & DISCUSSION

3.1. Tensile Test Results

Tensile test results are taken as the stroke vs force graph of the 2 samples produced for each specimen. Afterwards, using Equation 2.2, the stroke strain was divided by the force and the cross-sectional area, and the pressure applied to the surface was found and a stress-strain graph was created.

The yield strengths of the material were found by using the 2 percent method on the stress-strain graph. Ultimate tensile strength is marked as the max point on the chart.

Young's Modulus was found using Equation 2.3 and tabulated

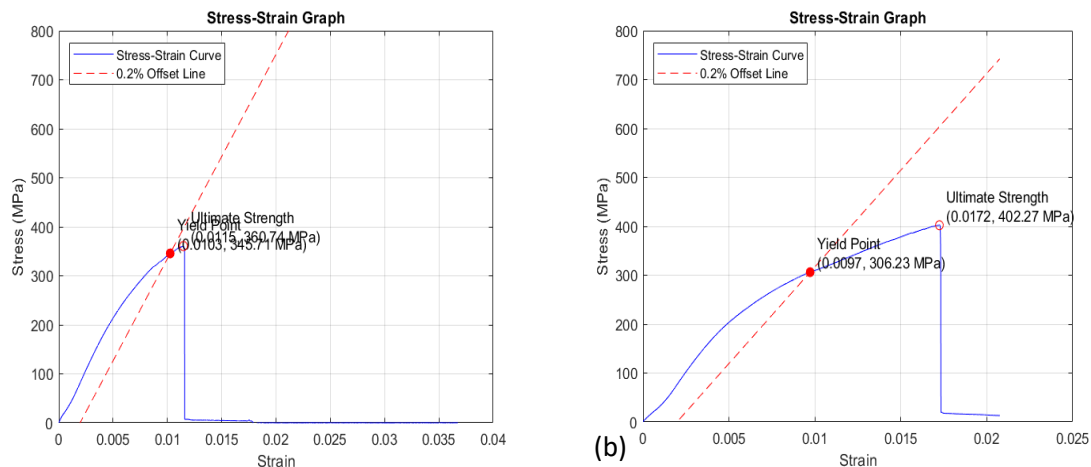


Figure 3.1. Composite No-4 Stress-Strain Graph (a) Sample 1; (b) Sample 2

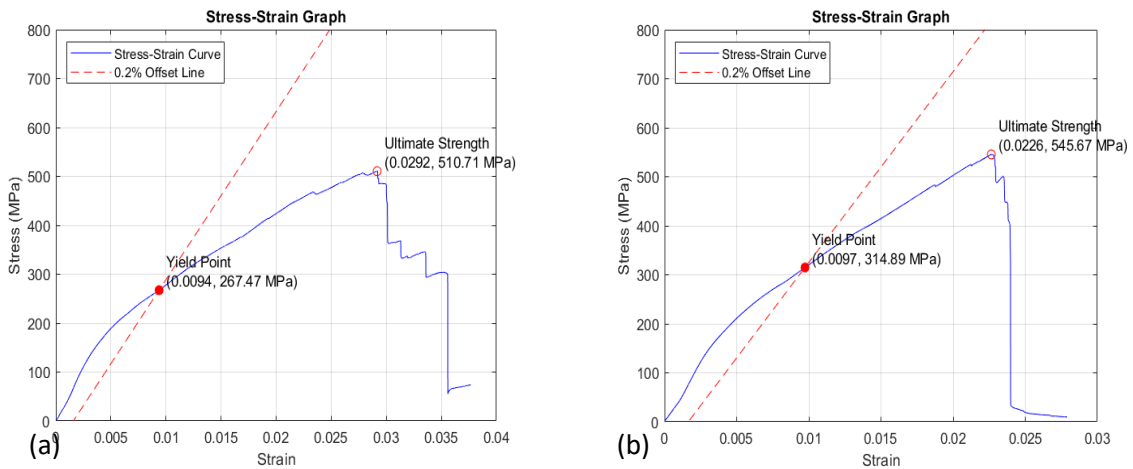


Figure 3.2. Composite No-3 Stress-Strain Graph (a) Sample; 1 (b) Sample 2.

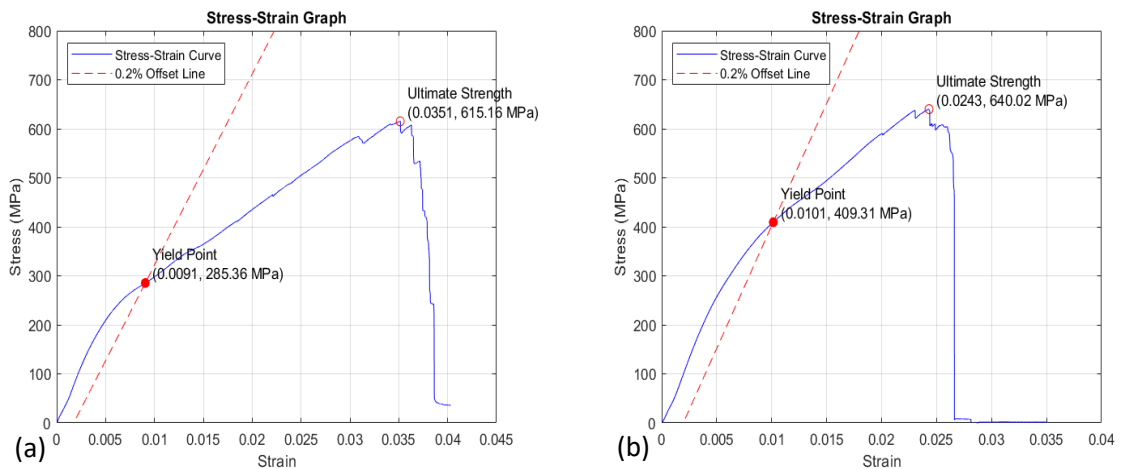


Figure 3.3. Composite No-2 Stress-Strain Graph (a) Sample 1; (b) Sample 2.

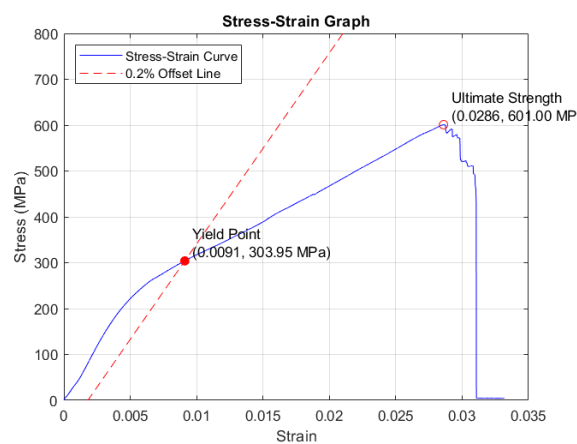


Figure 3.4. Composite No-1 Stress-Strain Graph Sample 1

Table 3.1. Tensile strength validation of Composite No-4

Sample No	Ultimate Tensile Strength (MPa)	Yield Strength (MPa)	Yield Strain	Young's Modulus (GPa)
1	360.74	345.71	0.0103	33.56
2	402.27	306.23	0.0097	31.57

Table 3.2. Tensile strength validation of Composite No-3

Sample No	Ultimate Tensile Strength (MPa)	Yield Strength (MPa)	Yield Strain	Young's Modulus (GPa)
1	510.71	267.47	0.0094	28.45
2	545.67	314.89	0.0097	32.46

Table 3.3. Tensile strength validation of Composite No-2

Sample No	Ultimate Tensile Strength (MPa)	Yield Strength (MPa)	Yield Strain	Young's Modulus (GPa)
1	615.16	285.36	0.0091	31.36
2	640.02	409.31	0.0101	40.53

Table 3.4. Tensile strength validation of Composite No-1

Sample No	Ultimate Tensile Strength (MPa)	Yield Strength (MPa)	Yield Strain	Young's Modulus (GPa)
1	601.00	303.95	0.0091	33.40

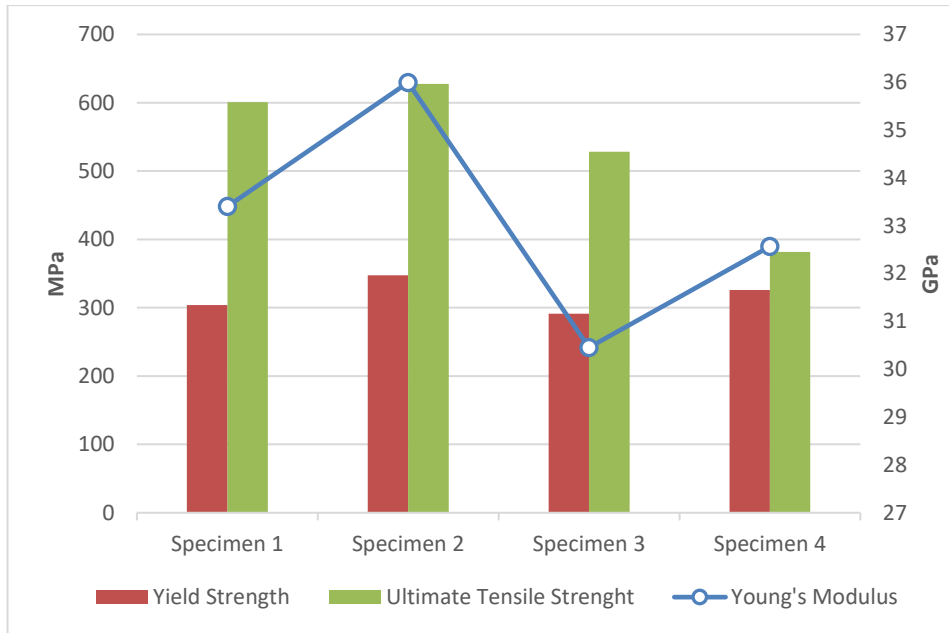


Figure 3.5. Average values of tensile strength properties of each composite

The graphic above shows four specimens. These samples contain nanoparticles in different proportions. The nanoparticles used are SiO_2 and TiO_2 . SiO_2 and TiO_2 nanoparticles were mixed in a mass ratio of one (1/1) and used in this way. No nanoparticles were used in Specimen 1. In Specimen 2, the ratio of the mass of the nanoparticle mixture to the entire sample is 0.01. In Specimen 3, the ratio of the mass of the nanoparticle mixture to the sample is 0.02. And finally, in specimen 4, the nanoparticle mixture mass ratio is 0.04. As can be understood from here, we wanted to observe how the mechanical properties would change in the tests we conducted by doubling the ratio of nanoparticle mass in each sample. The graph above shows the yield strength, ultimate tensile strength and Young's Modulus values when we apply the tensile test to the specimens. The image is a bar and line graph showing the mechanical properties of four different samples. The details of the chart are as follows:

- Yield strength (in MPa) is represented by red bars.
- Ultimate Tensile strength (in MPa) is represented by green bars.
- Young's modulus (in GPa) is represented by a blue line graph with circle markers.

On the x-axis, samples are ranked from 1 to 4. The left y-axis measures Yield strength and Ultimate tensile strength in MPa (from 0 to 700 MPa). The right y-axis measures Young's modulus in GPa (from 27 to 37 GPa).

Specimen 1 shows intermediate values for both types of strength and a higher value for Young's Modulus. Specimen 2 has the highest tensile strength and a peak in Young's Modulus. Specimen 3 shows a reduction in Tensile strength and a significant decrease in young modulus compared to Specimen 2. Specimen 4 shows similar values to Specimen 1 for

strengths and an intermediate value for young's modulus. Ultimate tensile strengths changed by +4.33%, -12.15%, -45.34% compared to the 0% particle added sample, respectively.

In composites with a high particle-to-mass ratio, aggregation may have occurred as a result of the particles not being distributed homogeneously. As a result, gaps were created between the carbon fibers, and these gaps resulted in a decrease in the tensile strength of the material.

3.2. Theoretical Results of Tensile Properties

The Mechanical Properties of a Unidirectional Lamina values found in the technical documents of the carbon-fiber used are processed in MATLAB code and what the Mechanical Properties of a Unidirectional Lamina will be if the laminates are arranged in the determined orientation is stated in the tables below.

Where mechanical properties are:

Table 3.5 Mechanical Properties of Epoxy/Carbon Fiber Composite

Mechanical Properties	Metric
Longitudinal elastic modulus (GPa)	70-75
Transverse elastic modulus (GPa)	5.5-6.5
Poisson's ratios	0.28
Shear modulus (GPa)	5-6
Ultimate longitudinal tensile strength (MPa)	600-750
Ultimate longitudinal compressive strength (MPa)	20-30
Ultimate transverse tensile strength (MPa)	100-150
Ultimate in-plane shear strength (MPa)	30-40

Table 3.6. Midplane Strains and Curvatures

ϵ_{0x}	ϵ_{0y}	ϵ_{0z}	κ_z	κ_z	κ_x
1.0964×10^{-9}	-2.8555×10^{-10}	0	0	0	0

Table 3.7. Elastic Constants for this laminate

E1	E2	G _{xy}	v _{xy}	v _{yx}
33.78 GPa	26.96 GPa	10.87 GPa	2.6045×10^{-1}	2.0786×10^{-1}

Physical Properties of Laminate A:

Table 3.8. Global Stresses (Pa)

Ply no.	Position	σ_x	σ_y	τ_{xy}
1 (0°)	Top	7.6779×10^1	1.1862×10^{-1}	0
	Bottom	7.6779×10^1	1.1862×10^{-1}	0
2 ($+45^\circ$)	Top	2.2937×10^1	9.1177×10^0	0
	Bottom	2.2937×10^1	9.1177×10^0	0
3 (-45°)	Top	2.2937×10^1	9.1177×10^0	0
	Bottom	4.2837×10^1	-2.2967×10^1	0
4 (90°)	Top	4.2837×10^0	-1.8413×10^0	0
	Bottom	4.2837×10^0	-1.8413×10^0	0
5 (0°)	Top	7.6779×10^1	1.1862×10^{-1}	0
	Bottom	7.6779×10^1	1.1862×10^{-1}	0
6 (90°)	Top	4.2837×10^1	-2.2967×10^1	0
	Bottom	1.9927×10^1	1.1539×10^1	0
7 (-45°)	Top	2.2937×10^1	9.1177×10^0	0
	Bottom	2.2937×10^1	9.1177×10^0	0
8 ($+45^\circ$)	Top	2.2937×10^1	9.1177×10^0	0
	Bottom	2.2937×10^1	9.1177×10^0	0
9 (0°)	Top	7.6779×10^1	1.1862×10^{-1}	0
	Bottom	7.6779×10^1	1.1862×10^{-1}	0

Table 3.9. Global Strains

Ply no.	Position	ϵ_x	ϵ_y	γ_{xy}
1 (0°)	Top	1.0964×10^{-9}	-2.8555×10^{-10}	0
	Bottom	1.0964×10^{-9}	-2.8555×10^{-10}	0
2 ($+45^\circ$)	Top	1.0964×10^{-9}	-2.8555×10^{-10}	0
	Bottom	1.0964×10^{-9}	-2.8555×10^{-10}	0
3 (-45°)	Top	1.0964×10^{-9}	-2.8555×10^{-10}	0
	Bottom	1.0964×10^{-9}	-2.8555×10^{-10}	0
4 (90°)	Top	1.0964×10^{-9}	-2.8555×10^{-10}	0
	Bottom	1.0964×10^{-9}	-2.8555×10^{-10}	0
5 (0°)	Top	1.0964×10^{-9}	-2.8555×10^{-10}	0
	Bottom	1.0964×10^{-9}	-2.8555×10^{-10}	0
6 (90°)	Top	1.0964×10^{-9}	-2.8555×10^{-10}	0
	Bottom	1.0964×10^{-9}	-2.8555×10^{-10}	0
7 (-45°)	Top	1.0964×10^{-9}	-2.8555×10^{-10}	0
	Bottom	1.0964×10^{-9}	-2.8555×10^{-10}	0
8 ($+45^\circ$)	Top	1.0964×10^{-9}	-2.8555×10^{-10}	0
	Bottom	1.0964×10^{-9}	-2.8555×10^{-10}	0
9 (0°)	Top	1.0964×10^{-9}	-2.8555×10^{-10}	0
	Bottom	1.0964×10^{-9}	-2.8555×10^{-10}	0

Table 3.10. Local Stresses (Pa)

Ply no.	Position	σ_1	σ_2	τ_{12}
1 (0°)	Top	7.6779×10^1	1.1862×10^{-1}	0
	Bottom	7.6779×10^1	1.1862×10^{-1}	0
2 ($+45^\circ$)	Top	2.9183×10^1	2.8718×10^0	-6.9096×10^0
	Bottom	2.9183×10^1	2.8718×10^0	-6.9096×10^0
3 (-45°)	Top	2.9183×10^1	2.8718×10^0	6.9096×10^0
	Bottom	2.9183×10^1	2.8718×10^0	6.9096×10^0
4 (90°)	Top	-1.8413×10^1	5.6249×10^0	0
	Bottom	-1.8413×10^1	5.6249×10^0	0
5 (0°)	Top	7.6779×10^1	1.1862×10^{-1}	0
	Bottom	7.6779×10^1	1.1862×10^{-1}	0
6 (90°)	Top	-1.8413×10^1	5.6249×10^0	0
	Bottom	-1.8413×10^1	5.6249×10^0	0
7 (-45°)	Top	2.9360×10^1	2.1050×10^0	6.9096×10^0
	Bottom	2.9360×10^1	2.1050×10^0	6.9096×10^0
8 ($+45^\circ$)	Top	2.9360×10^1	2.1050×10^0	-6.9096×10^0
	Bottom	2.9360×10^1	2.1050×10^0	-6.9096×10^0
9 (0°)	Top	7.6779×10^1	1.1862×10^{-1}	0
	Bottom	7.6779×10^1	1.1862×10^{-1}	0

Table 3.11. Local Strains

Ply no.	Position	ϵ_1	ϵ_2	γ_{12}
1 (0°)	Top	1.0964×10^{-9}	-2.8555×10^{-10}	0
	Bottom	1.0964×10^{-9}	-2.8555×10^{-10}	0
2 ($+45^\circ$)	Top	4.0541×10^{-10}	4.0541×10^{-10}	-1.3819×10^{-9}
	Bottom	4.0541×10^{-10}	4.0541×10^{-10}	-1.3819×10^{-9}
3 (-45°)	Top	4.0541×10^{-10}	4.0541×10^{-10}	1.3819×10^{-9}
	Bottom	4.0541×10^{-10}	4.0541×10^{-10}	1.3819×10^{-9}
4 (90°)	Top	-2.8555×10^{-10}	1.0964×10^{-9}	0
	Bottom	-2.8555×10^{-10}	1.0964×10^{-9}	0
5 (0°)	Top	1.0964×10^{-9}	-2.8555×10^{-10}	0
	Bottom	1.0964×10^{-9}	-2.8555×10^{-10}	0
6 (90°)	Top	-2.8555×10^{-10}	1.0964×10^{-9}	0
	Bottom	-2.8555×10^{-10}	1.0964×10^{-9}	0
7 (-45°)	Top	4.0541×10^{-10}	4.0541×10^{-10}	1.3819×10^{-9}
	Bottom	4.0541×10^{-10}	4.0541×10^{-10}	1.3819×10^{-9}
8 ($+45^\circ$)	Top	4.0541×10^{-10}	4.0541×10^{-10}	-1.3819×10^{-9}
	Bottom	4.0541×10^{-10}	4.0541×10^{-10}	-1.3819×10^{-9}
9 (0°)	Top	1.0964×10^{-9}	-2.8555×10^{-10}	0
	Bottom	1.0964×10^{-9}	-2.8555×10^{-10}	0

When the theoretically obtained E1 value of 33.78 GPa is compared with the

Longitudinal Young's Modulus of 33.4 GPa of the specimen with 0% particles, a difference of -1% is observed. In this case, the local and global stress strain values shown in the tables can be evaluated with a tolerance of 1%.

3.3. Charpy Impact Test Results

The impact test results of 2 specimens produced for each sample were recorded as time and force graphs. These graphs provided significant information about how the material behaves under sudden loading conditions. Subsequently, using the impact energy, the fracture toughness of each specimen was calculated; this is a measure of the material's ability to resist crack propagation. Additionally, an energy absorption graph was created to show how much energy the material can absorb before breaking [22].

The fracture strengths of the material were determined from the highest energy absorption point in the impact energy graph. This peak represents the point at which the material begins to fracture after it can no longer absorb more energy. The ultimate impact strength was marked on the graph as the maximum energy the material can withstand before breaking [23].

The findings from this analysis were systematically compiled into a table, enabling a clear comparison.

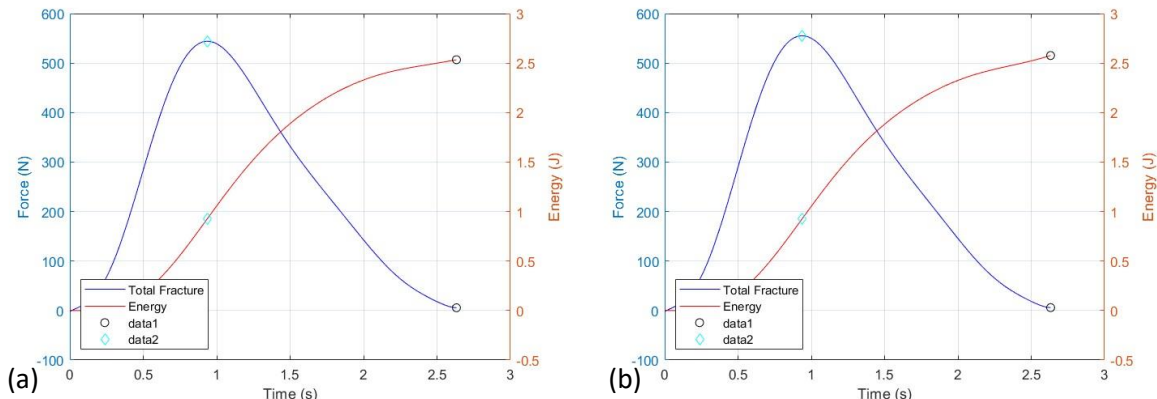


Figure 3.6. Composite No-4 Time vs Force and Energy Graph (a) Sample 1; (b) Sample 2.

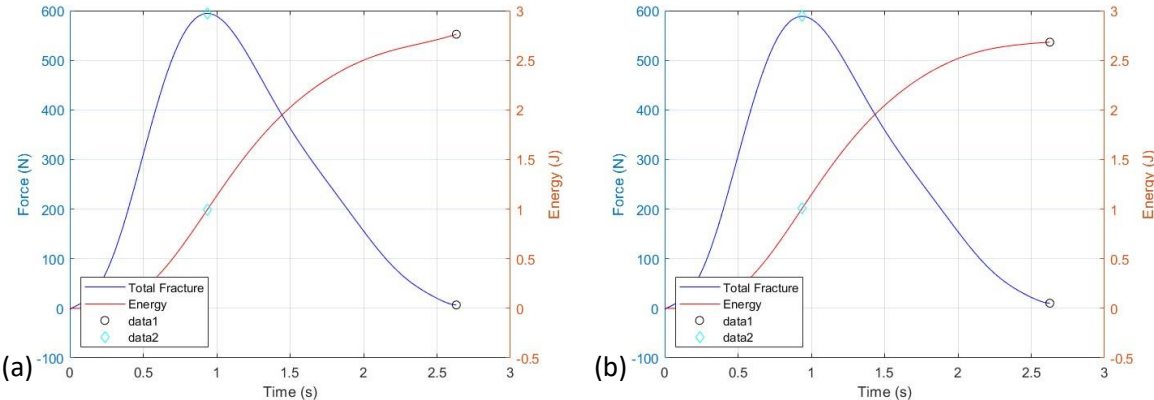


Figure 3.7. Composite No-3 Time vs Force and Energy Graph (a) Sample 1; (b) Sample 2.

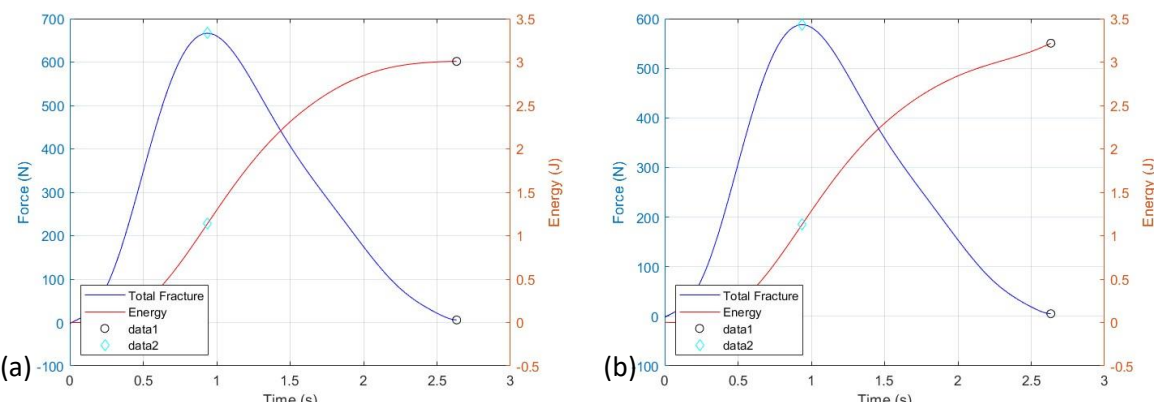


Figure 3.8. Composite No-2 Time vs Force and Energy Graph (a) Sample 1; (b) Sample 2.

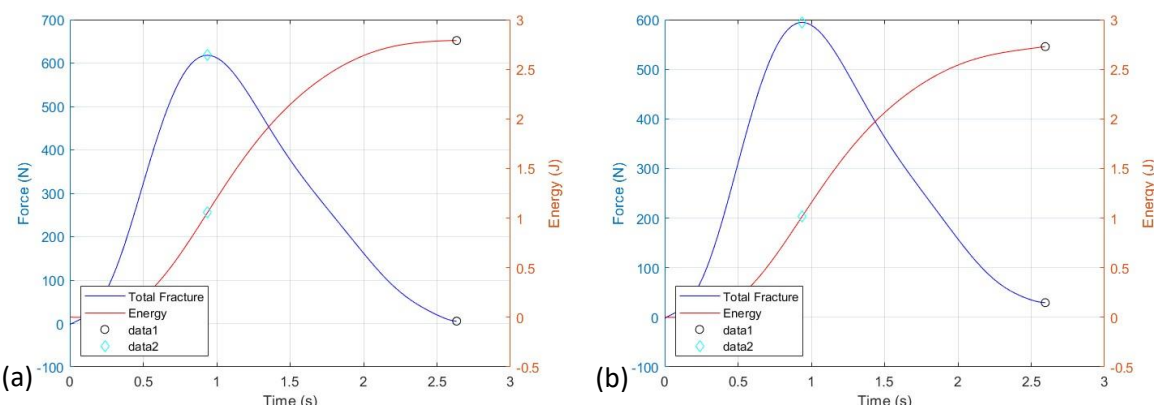


Figure 3.9. Composite No-1 Time vs Force and Energy Graph (a) Sample 1; (b) Sample 2.

Table 3.12. Impact strength validation of Composite No-4

Sample No	Crack Initiation Impact Strength (J/m ²)	Crack Propagation Impact Strength (J/m ²)	Total Charpy Impact Strength (J/m ²)
1	38.66792	66.90708	105.575
2	38.52917	68.81667	107.3458

Table 3.13. Impact strength validation of Composite No-3

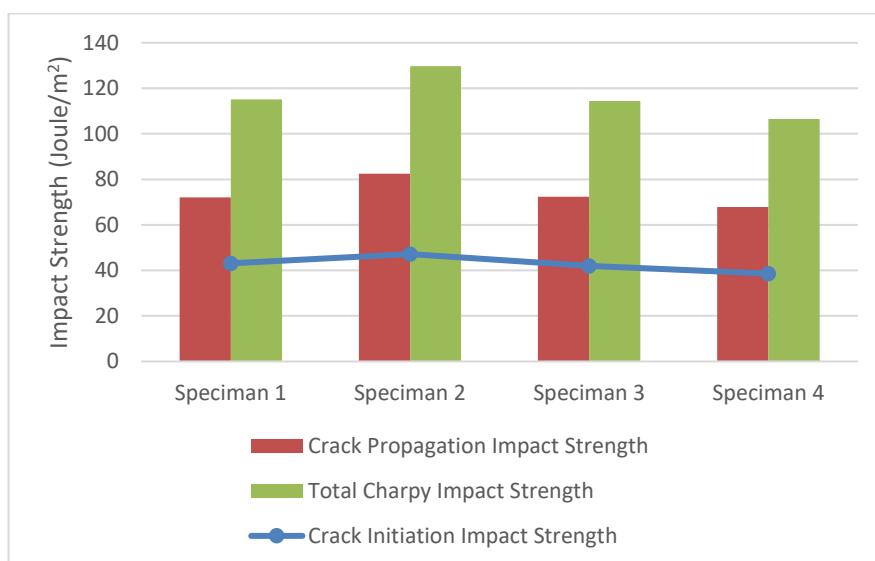
Sample No	Crack Initiation Impact Strength (J/m ²)	Crack Propagation Impact Strength (J/m ²)	Total Charpy Impact Strength (J/m ²)
1	42.24167	74.925	117.1667
2	41.87083	69.90833	111.7792

Table 3.14. Impact strength validation of Composite No-2

Sample No	Crack Initiation Impact Strength (J/m ²)	Crack Propagation Impact Strength (J/m ²)	Total Charpy Impact Strength (J/m ²)
1	47.34583	77.98333	125.3292
2	46.97917	87.06667	134.0458

Table 3.15. Impact strength validation of Composite No-1

Sample No	Crack Initiation Impact Strength (J/m ²)	Crack Propagation Impact Strength (J/m ²)	Total Charpy Impact Strength (J/m ²)
1	43.9125	72.325	116.2375
2	42.24167	71.70417	113.9458

**Figure 3.10** Average values of impact strength properties of each composite

Carbon fiber composite, prepared with an epoxy mixture mixed with SiO₂ and TiO₂ particles, prevents the formation of micro cracks in the composite matrix of the particles and provides impact resistance that will make it difficult for tearing to progress in the cracks formed. The strong interfacial interactions of the particles with the epoxy increase the impact resistance of the composite [24].

When we look at crack propagation resistance, Specimen 2 is the sample with the most ductile properties. In this case, Specimen 4 is the specimen with the most brittle feature. The reason for this may be that the particles aggregate in the epoxy mixture with a high percentage of particles and disrupt the homogeneity of the composite. Total Charpy strengths changed by +12.6%, -0.5%, -7.5% compared to the 0% particle added sample, respectively.

4. FEASIBILITY & COST ANALYSIS

The production costs of the composites produced within the scope of the project were analyzed.

Table 4.1. Cost analysis of the project.

		Manufacturing Costs	Number or Amount	Cost
Manufacturing Cost	Material Cost	Carbon Plies	1m ²	₺ 843.88
		Resin	250 g	₺ 214.22
		Hardener	125 g	₺ 107.11
		Vacuum Sealing Tape	15 m	₺ 346.73
		Peel Ply	1 m ²	₺ 113.74
		Vacuum Bag	4.5m ²	₺ 440.28
		Breather Cloth	1.5m ²	₺ 58.70
		SiO ₂ particle	5.8 g	₺ 26.42
		TiO ₂ particle	5.8 gr	₺ 2.51
	Capital Cost	Pump	1	-
		Teflon	1	-
		Sonicator	1	-
		Infusion Vacuum Hose	1 m	₺ 26.05
		Valve	2	₺ 183.46

Industry Costs	Cutting and Finishing Cost	Labor Cost	16	₺ 500
			TOTAL	₺ 2863.1

Adding different amounts of nanoparticles to carbon fiber epoxy composites aims to improve the mechanical properties of the material and find the most suitable value. The performance of the composites produced by adding nanoparticles (0, 1%, 2%, 4%) was evaluated with tensile and impact tests. According to the analysis results, it is shown that adding nanoparticles at low rates increases the strength of the composite material and the costs are at an acceptable level. As a result, it can be said that the project is economically and technically feasible.

5. CONCLUSION & FUTURE WORKS

In this undergraduate thesis, carbon-fiber epoxy composites containing four different nanoparticle weights were produced. The orientation of these composites was optimized by comparing them in different sequences and the appropriate ply orientation $[0^\circ / +45^\circ / -45^\circ / 90^\circ / 0^\circ / 90^\circ / -45^\circ / +45^\circ / 0^\circ]$ was found. Composites that did not contain nanoparticles and that contained nanoparticles in different mass ratios were tested, and then it was examined how the ratio of nanoparticles in the composite affected its mechanical properties. While examining its effect on mechanical properties, tensile test and Charpy impact test were applied. In the tensile test, the composite containing 1% $\text{SiO}_2\text{-TiO}_2$ particles gave the best results, that is, a 4.33% increase in Ultimate tensile strength was observed compared to the composite containing no nanoparticles. However, a decrease in the mechanical properties of composites containing 2% and 4% nanoparticles was observed compared to the composite containing no nanoparticles. In the impact test, the inclusion of nanoparticles in the composites increased the impact resistance by preventing the formation of micro cracks and making it difficult for the cracks to propagate. Sample 2 has the most ductile properties, while Sample 4 has the most brittle properties. This may be due to the high particle ratio disrupting the homogeneity of the composite. Total Charpy strengths changed by +12.6%, -0.5%, -7.5% compared to the 0% particle added sample, respectively. It was observed that the mechanical properties of the produced composites decreased significantly after the ratio of nanoparticles mixed with epoxy exceeded the optimum value. The reason may be that aggregation occurs in epoxies with high particles in mass, and this agglomeration disrupts the homogeneity of the composite and disrupts the load distribution. Therefore, the

particle ratio and distribution should be kept at the appropriate rate.

For further studies, composites with different weight ratios such as 0.5% can be produced and the optimum value can be found. In addition, composites can be analyzed with different tests such as three-point bending as well as tensile and notch impact tests.

6. REFERENCES

- [1] F. Han, Y. Yan, J. Ma, Experimental Study and Progressive Failure Analysis of Stitched Foam-core Sandwich Composites Subjected to Low-velocity Impact, *Polym. Compos.* 39 (3) (2016) 624–635.
- [2] J. Wang, A.M. Waas, H. Wang, Experimental and numerical study on the low velocity impact behavior of foam-core sandwich panels, *Compos. Struct.* 96 (2013) 298–311.
- [3] Byung Chul Kim, Sang Wook Park, Dai Gil Lee, Fracture toughness of the nano particle reinforced epoxy composite, *Compos. Struct.* 86 (2008) 69–77.
- [4] A. Kandelbauer, Processing. InHandbook of Thermoset Plastics, 3rd ed.; Dodiuk, H., Goodman, S. H., Eds.;WilliamAndrew, 2014; pp 739– 753. [Crossref],GoogleScholar.
- [5] M. Zhang, H. Zeng, L. Zhang, G. Lin, R. K. Y. Li (1993) Fracture characteristics of discontinuous carbon fibre-reinforced PPS and PES-C composites, *Polym. Polym. Compos.* 1,357.
- [6] F. Heutling, H. E. Franz, K. Friedrich (1998) Photomicrographic fracture analysis of the delamination propagation in cyclic loaded thermosetting carbon fiber-reinforced composites, *Materialwissenschaften und Werkstofftechnik* 29, 239 (in German).
- [7] B. Wetzel, F. Haupert, M. Z. Rong (2002) Nanoparticle-reinforced composites: preparation, structure, properties, Proc. 81h Natl. Symp. SAMPE, Deutschland e.V., Kaiserslautern (in German).
- [8] B. Suresha, G.S. Divya, G.Hemanth& H.M. Somashekhar (2021)Physico-Mechanical Properties of Nano Silica-Filled Epoxy- Based Mono and Hybrid Composites for Structural Applications.
- [9] Mohd Khirul Hafiz Muda, Faizal Mustapha, in Sustainable Composites for Aerospace Applications, 2018 Composite patch repair using natural fiber for aerospace applications, sustainable composites for aerospace applications
- [10] Rong Z, Sun W, Xiao H, Jiang G. “Effects of nano-SiO₂ particles on the mechanical and microstructural properties of ultra-high performance cementitious composites”. *Cement and Concrete Composites*, 56, 25-31, 2015.
- [11] Tutunchi A, Kamali R and Kianvash A. Steel–epoxy composite joints bonded with nano TiO₂ reinforced structural acrylic adhesives. *J Adhes* 2015; 91(9): 663–676.

- [12] M. Landowski, G. Strugala, M. Budzik (2017) Impact damage in SiO₂ nanoparticle enhanced epoxy – Carbon fibre composites
- [13] Ahmed Sattar Jabbar Al-Zubaydi, Rana M Salih and Balqees M Al-Dabbagh. Effect of nano TiO₂ particles on the properties of carbon fiber-epoxy composites. Progress in Rubber Plastics and Recycling Technology 2021; Vol. 37(3) 216–232
- [14] Can TUNCER, Olcay Ersel CANYURT. The strength of glass fiber composite materials by inclusion of CaCO₃ and SiO₂ nanoparticles into resin 2022; Pamukkale Univ Muh Bilim Derg, 28(4), 493-498, 2022
- [15] Irisarri, F., Lasseigne, A., Leroy, F., & Le Riche, R. (2014). Optimal design of laminated composite structures with ply drops using stacking sequence tables. Composite Structures, 559-564.
- [16] Dangsheng X. Friction and wear properties of UHMWPE composites reinforced with carbon fibers. Mater Lett 2005; 59: 175–179. 7.
- [17] Molazemhosseini A, Tourani H, Khavandi A, et al. Tribological performance of PEEK based hybrid composites reinforced with short carbon fibers and nano silica. Wear 2013; 303(1–2): 397–404. 8.
- [18] Stoeffler K, Andjelic S, Legros N, et al. Polyphenylene sulfide (PPS) composites reinforced with recycled carbon fiber. Compos Sci Technol 2013; 84: 65–71.
- [19] Cox HL. “The elasticity and strength of paper and other fibrous materials”. British Journal of Applied Physics, 3(3), 72-79, 1952.
- [20] Carlo S. Mechanical and impact damage analysis on carbon/natural fiber hybrid composites: a review. Materials 2019; 12(3): 517–527.
- [21] American Society for Testing and Materials. “Standard Test Method for Tensile Properties of Polymer Matrix Composite Materials”. Pennsylvania, USA, D3039, 2014.
- [22] Tutunchi A, Kamali R and Kianvash A. Steel–epoxy composite joints bonded with nano TiO₂ reinforced structural acrylic adhesives. J Adhes 2015; 91(9): 663–676.
- [23] Can U and Kaynak C. Effects of micro-nano titania contents and maleic anhydride compatibilization on the mechanical performance of polylactide. Polym Composit 2020; 41(2): 600–613.
- [24] Fu S. “Effects of fiber length and fiber orientation distributions on the tensile strength of short-fiberreinforced polymers”. Composites Science and Technology,

7. APPENDIX

Matlab code of optimization of ply orientations:

```

clc;clear
format shortE
syms x

% Material properties for Carbon/epoxy
E1 = 70.0*10^9; % Longitudinal elastic modulus(Pa)
E2 = 5.5*10^9; % Transverse elastic modulus(Pa)
nu12 = 0.28; % Poisson's ratio
G12 = 5*10^9; % Shear modulus(Pa)
S_1T = 600*10^6; % Ultimate longitudinal tensile strength
S_1C= 600*10^6; % Ultimate longitudinal compressive strength
S_2T=20*10^6; % Ultimate transverse tensile strength
S_2C=120*10^6; % Ultimate transverse compressive strength
T_12=30*10^6; % Ultimate in-plane shear strength

% Layer properties
t=0.003; % Thickness(m)
n=9; % Number of Layer
h=t*n; % Total Thickness
theta=[0 45 -45 90 0 90 -45 45 0]; % Ply orientations (in degrees)
theta = theta*pi/180; % Ply orientation to radians

% Define local compliance matrix
S_local = [1/E1 -nu12/E1 0; -nu12/E1 1/E2 0; 0 0 1/G12];

%Calculation reduced transformed stiffness matrices
for i=1:1:n
c=cos(theta(1,i));
s=sin(theta(1,i));
T=[c^2 s^2 2*s*c;s^2 c^2 -2*s*c;-s*c s*c c^2-s^2]; % Transformation matrix
R=[1 0 0;0 1 0;0 0 2]; % Reuter matrix
Qcell{i}=inv(T)*inv(S_local)*R*T*inv(R); % Reduced transformed stiffness matrices
end

% Calculate locations of the ply surfaces
for i=0:1:n
h0=-h/2;
ht{i+1}=h0+i*t;
end

% Calculate A
for i=1:1:n
I{i}=Qcell{i}*(ht{i+1}-ht{i});

```

```

end

A=I{1}+I{2}+I{3}+I{4}+I{5}+I{6}+I{7}+I{8}+I{9};

% Calculate B
for i=1:1:n
    J{i}=Qcell{i}*(ht{i+1}^2-ht{i}^2);
end
B=(J{1}+J{2}+J{3}+J{4}+J{5}+J{6}+J{7}+J{8}+J{9})*0.5;

% Calculate D
for i=1:1:n
    K{i}=Qcell{i}*(ht{i+1}^3-ht{i}^3);
end
D=(K{1}+K{2}+K{3}+K{4}+K{5}+K{6}+K{7}+K{8}+K{9})*(1/3);

% Calculate midplane strains and curvatures
V=inv([A B;B D])*[1;0;0;0;0]; % Equation 4.29(Ny= 1000N/m)

fprintf("1. Midplane strains and curvatures\n");
fprintf('t\te0x \t\te0y \t\t\te0z\t\te\kappa z\t\te\kappa z\t\te\kappa x\n');
disp(V');
disp("-----");

%Determine the five effective elastic constants for this laminate.
%Laminate is symetrics
A_s=inv(A); % Equation 4.31
E_x= 1/(h*A_s(1,1)); % Equation 4.35
E_y= 1/(h*A_s(2,2)); % Equation 4.37
G_xy= 1/(h*A_s(3,3)); % Equation 4.39
v_xy= -A_s(1,2)/A_s(1,1); % Equation 4.42
v_yx= -A_s(1,2)/A_s(2,2); % Equation 4.45
Co=[E_x E_y G_xy v_xy v_yx];

fprintf("2. Determine the five effective elastic constants for this laminate.\n");
fprintf('t\Ex \t\tey \t\t\txy\t\txy\t\tyx\t\tyx\n');
disp(Co);
disp("-----");

% Calculate global lamina strains & global lamina stresses
for i=1:1:n

    Strain_Global{i} = [V(1,1);V(2,1);V(3,1)] + (ht{i})*[V(4,1);V(5,1);V(6,1)];
    Stress_Global{i}= Qcell{i}*Strain_Global{i};
end

for i=1:1:n
    po=int2str(i);
    fprintf("Global strains level %s ply\n",po);

```



```
solve(Sr,x);
sol(i) = max(round(solve(Sr,x)));
end

fprintf("Strength Ratios\n");
disp(max(sol));
disp("-----");
```